Copy No. _14_

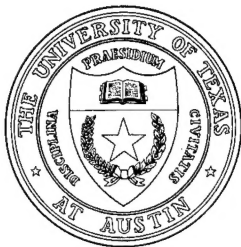# Bottom Grain Gas and Roughness Technique (BOGGART) Version 1.0: Bottom Backscatter Model User's Guide

Technical Report under Contract N00039-91-C-0082
TD No. 01A2049, Sensor and Environmental Support for MTEDS

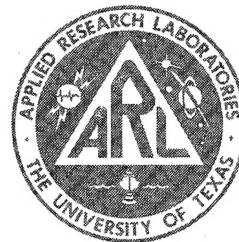Frank A. Boyle
Nicholas P. Chotiros

Applied Research Laboratories
The University of Texas at Austin
P. O. Box 8029   Austin, TX 78713-8029

2 October 1995

Technical Report

19960708 085

DTIC QUALITY INSPECTED 1

UNCLASSIFIED

REPORT DOCUMENTATION PAGE

Form Approved
OMB No. 0704-0188

Public reporting burden for this collection of Information is estimated to average 1 hour per response, Including the time for reviewing Instructions, searching existing data sources, gathering and maintaining the data needed, and completing and reviewing the collection of Information. Send comments regarding this burden estimate or any other aspect of this collection of Information, Including suggestions for reducing this burden, to Washington Headquarters Services, Directorate for Information Operations and Reports, 1215 Jefferson Davis Highway, Suite 1204, Arlington, VA 22202-4302, and to the Office of Management and Budget, Paperwork Reduction Project (0704-0188), Washington, DC 20503.

1. AGENCY USE ONLY (Leave blank)	2. REPORT DATE	3. REPORT TYPE AND DATES COVERED
	2 Oct 95	technical

4. TITLE AND SUBTITLE
Bottom Grain Gas and Roughness Technique (BOGGART) Version 1.0: Bottom Backscatter Model User's Guide, Technical Report under Contract N00039-91-C-0082, TD No. 01A2049, Sensor and Environmental Support for MTEDS

5. FUNDING NUMBERS
N00039-91-C-0082,
TD No. 01A2049

6. AUTHOR(S)
Boyle, Frank A.   Chotiros, Nicholas P.

7. PERFORMING ORGANIZATION NAMES(S) AND ADDRESS(ES)
Applied Research Laboratories
The University of Texas at Austin
P.O. Box 8029
Austin, Texas 78713-8029

8. PERFORMING ORGANIZATION REPORT NUMBER
ARL-TR-95-27

9. SPONSORING/MONITORING AGENCY NAME(S) AND ADDRESS(ES)
Naval Research Laboratory
Stennis Space Center, MS 39529-5004

Space and Naval Warfare Systems
  Command
Department of the Navy
Arlington, VA 22245-5200

10. SPONSORING/MONITORING AGENCY REPORT NUMBER

11. SUPPLEMENTARY NOTES

12a. DISTRIBUTION/AVAILABILITY STATEMENT
Approved for public release; distribution is unlimited.

12b. DISTRIBUTION CODE

13. ABSTRACT (Maximum 200 words)

A user's guide for ARL:UT's marine sediment acoustic backscatter model has been developed. The model, named BOGGART (Bottom Grain Gas and Roughness Technique), is a three-component model which computes the total backscattering strength as an incoherent sum of contributions from three components. They are (1) scattering from sediment grains, (2) scattering from trapped gas bubbles within the sediment, and (3) scattering from interface roughness. The grain scattering is modeled empirically in lieu of a theoretical model which is under development. The gas bubble and roughness scattering components are theoretical. Acoustic propagation in the sediment is modeled by way of the Biot theory for poroelastic media. This report describes BOGGART's program structure, as well as its input and output file management. It is intended to suffice as a user's description of the model's operation.

14. SUBJECT TERMS

backscatter	grains	sand
Biot theory	porous medium	seafloor
gas bubbles	roughness	sediment

15. NUMBER OF PAGES
35

16. PRICE CODE

17. SECURITY CLASSIFICATION OF REPORT	18. SECURITY CLASSIFICATION OF THIS PAGE	19. SECURITY CLASSIFICATION OF ABSTRACT	20. LIMITATION OF ABSTRACT
UNCLASSIFIED	UNCLASSIFIED	UNCLASSIFIED	SAR

NSN 7540-01-280-5500

UNCLASSIFIED

Standard Form 298 (Rev. 2-89)
Prescribed by ANSI Std. 239-18
298-102

This page intentionally left blank.

TABLE OF CONTENTS

This page intentionally left blank.

LIST OF FIGURES

This page intentionally left blank.

1. INTRODUCTION

Acoustic backscatter from the seafloor has generated considerable interest over the past several decades. The importance of seabed acoustics has recently grown due to current emphasis on mine warfare in the littoral environment. Since there is at present no general agreement on the physics of the scattering process, a lot of models exist, based on several different hypothetical scattering mechanisms. They include models based on scattering at the sediment interface, like those of Patterson[1] and Clay and Medwin,[2] as well as the volume scattering models of Nolle et al.,[3] Stockhausen,[4] and Ivakin and Lysanov.[5] Jackson et al.[6-8] developed a two-component model that treats interface roughness scattering and volume scattering separately. Applying this model to several sites suggests that both components are important, each dominating the total backscatter prediction in half of six cases.

Jackson's model uses six parameters to characterize the seabed, two of which describe the interface roughness and three of which describe acoustic propagation through the sediment, modeled as an acoustic fluid. The remaining parameter is an empirically determined quantity which specifies the level of volume scattering within the sediment. No attempt is made to specify the actual volume scattering mechanisms involved.

In 1990, Chotiros[9] began a comprehensive compilation of all available shallow grazing angle backscatter data published in the literature. The results appeared to show some statistically significant trends that suggest specific volume scattering mechanisms, which might be modeled physically. Two hypothetical scattering mechanisms, involving scattering from sediment grains and from trapped bubbles, appear to fit the general trends in the data. At present the data set is expanding and the trends remain.

In 1992 the results of three acoustic penetration experiments at sea[10,11] and in the laboratory[12] became available. They suggested that sandy sediments might best be modeled structurally via the Biot poroelastic theory, particularly for high frequencies and shallow grazing angles.

1

In 1993 development of a new backscatter model[13] was begun with the intention of taking advantage of the most recent experimental information. The result is ARL:UT's current bottom backscatter model called BOGGART. It is intended for minehunting applications and therefore optimized for shallow grazing angle, high frequency behavior. Like Jackson's model, BOGGART includes volume and interface scattering components. It is different in its modeling of the sediment's structure and in the scattering mechanisms.

BOGGART is unique among current scattering models in two important ways. First, the sediment is modeled structurally via the Biot theory. Second, the volume scattering is modeled physically rather than empirically. BOGGART consists of three modular components that predict partial scattering strengths due to sediment grains, gas bubbles, and interface roughness. Hence the name, which is an acronym for "bottom grain gas and roughness technique".

This report is intended to serve as a user's manual. Section 2 is an overview of the theory. In Section 3, BOGGART's structure is described. Section 4 is a user's description of the model's operation.

2. OVERVIEW OF THEORY

This section discusses the underlying concepts upon which BOGGART is built. As stated in the introduction, BOGGART differs from other current backscatter models because it incorporates the Biot theory to describe the seabed's structure, and because the volume scattering mechanisms are modeled physically rather than empirically. Section 2.1 discusses the Biot theory's significance in modeling backscatter. Section 2.2 explains BOGGART's physical scattering mechanisms.

2.1 BIOT THEORY

The Biot theory differs from other sediment theories in that it treats the sediment as a two-phase medium, consisting of a solid skeletal structure of sediment grains, through which a pore fluid flows. There exist two compressional waves, one consisting of pore fluid and grains moving in phase and a second consisting of the pore fluid and grains moving against one another out of phase. The first of these waves propagates fastest and is called the Biot fast wave; the other is called the Biot slow wave. Slow waves generally attenuate rapidly in comparison with fast waves and are therefore considered negligible. In general, therefore, sediments are modeled with simpler one-phase models, such as elastic or fluid models.

Recent experiments suggest that there are important special cases in which slow waves are not negligible, making the Biot theory most applicable. In these experiments, accomplished both at sea and in the laboratory, a slow acoustic wave was observed in sandy sediment with sound speeds near 1200 m/s. The wave was significant at frequencies greater than 10 kHz and grazing angles less than 20°. The existence of this wave cannot be explained via fluid or elastic theories, but can be modeled as a Biot slow wave with a reasonable set of input parameters.

Measurements of normal incidence reflection coefficients also suggest that sandy sediment is structured as a Biot medium. Figure 2.1 shows several such measurements, alongside theoretical values based on Biot and elastic theory. The Biot model appears to be most consistent with the measurements.
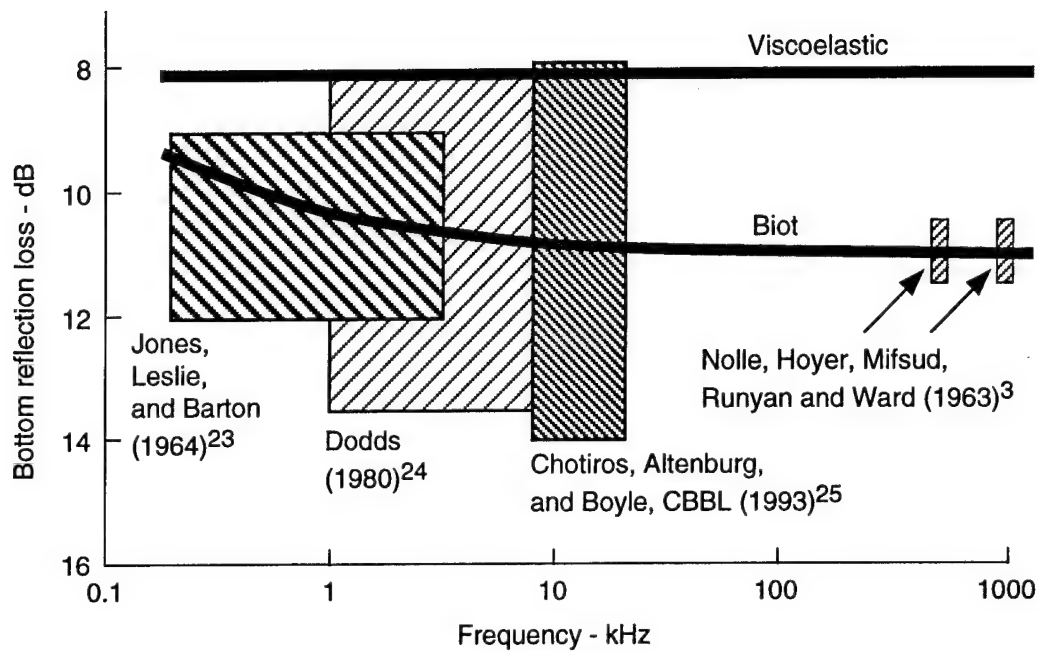
Figure 2.1
Comparison of published normal incidence reflection
measurements with viscoelastic and Biot theories.

The Biot theory used by BOGGART was originally formulated by Stern, Bedford, and Millwater.[14] Its incorporation in the model is described in Ref. 13.

2.2   SEDIMENT SCATTERING MECHANISMS

Figure 2.2 is a plot of all shallow grazing backscatter measurements available in the literature. This collection was compiled by Chotiros[9] and includes data from the USA, Canada, the UK, and Russia, beginning with some measurements recorded by Urick in the 1950s. Each data point represents a backscattering strength measurement over sediment at a grazing angle of 10°. The data span a broad range between an upper limit defined by Lambert's rule and energy conservation, and a lower limit defined by Nolle's experiments[3] over finely graded and degassed laboratory sands. An outstanding feature of Nolle's data is that the backscattering strength increases steadily with normalized grain size (grain diameter/wavelength).

If the data points are grouped according to the site they were collected from, two trends appear, shown in Fig. 2.3. In this figure, data points from a common site are connected with lines. In group 1, the backscattering strength increases with normalized grain size, just as was the case for Nolle's data over degassed sands. This dependence of the scattering strength on the size of the sediment grain suggests that the grains are involved in the scattering process. In group 2, the backscattering strength appears to have a relative maximum when the grain diameter is about $10^{-2.5}$ wavelengths. This is close to the resonance diameter of gas bubbles in water, suggesting that trapped bubbles in resonance might be a dominant mechanism.

BOGGART's hypothesis is that the shallow grazing angle scattering data of Figs. 2.2 and 2.3 are dominated by two scattering mechanisms: grain scattering, which dominates the data of group 1, and bubble scattering, which dominates group 2. At larger grazing angles, it is possible that interface roughness might become important. BOGGART models these three scattering mechanisms in separate modules, described below.
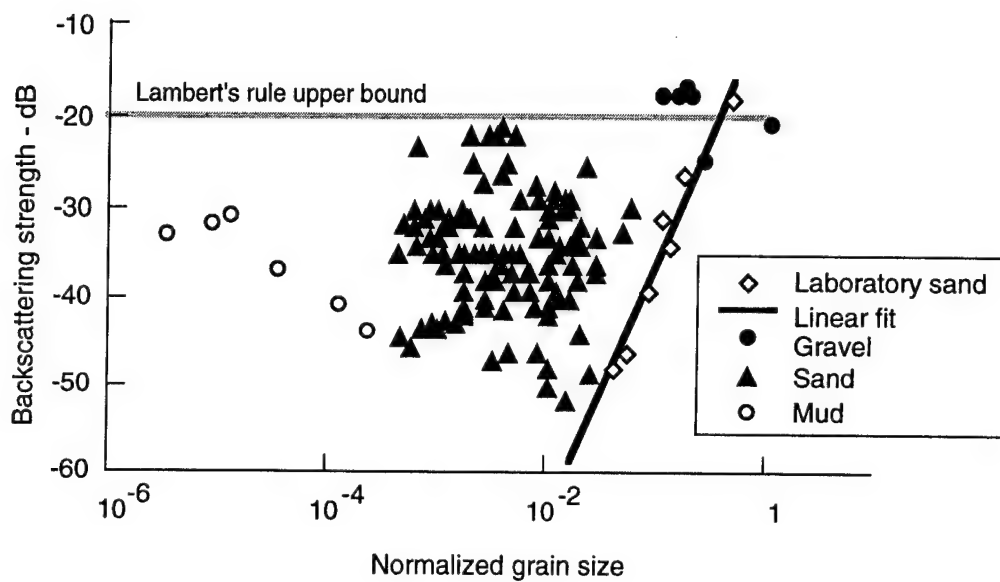
Figure 2.2
Experimental measurements of bottom backscattering strength as a function of grain size at a grazing angle of 10°, from all published sources.
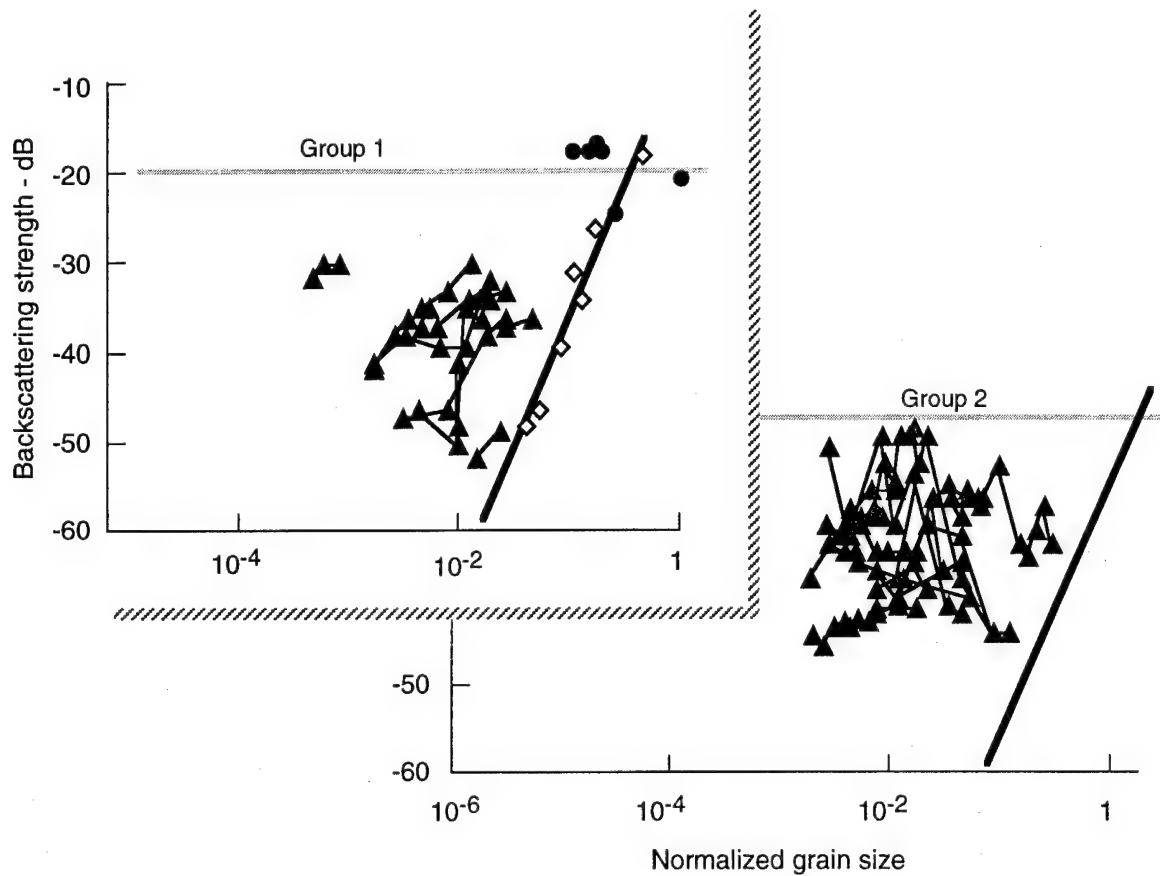
**Figure 2.3
Experimental measurements of bottom backscattering strength
as a function of grain size at a grazing angle
of 10°, groups 1 and 2.**

7

2.2.1 Sediment Grains

A theoretical model for acoustic scattering from sediment grains is currently under development.[15] It will be based on the Biot theory[14,16-18] for acoustic propagation through fluid saturated porous media, with a modification that includes the effects of scattering. In lieu of this scattering model, which is not complete, BOGGART models sediment grain scattering empirically, based on experimental data measured by Nolle et al.[3] The expression for backscattering strength is

$$BS_g = 30 \min \left[-0.4623, \log \left(\frac{dk}{2\pi} \right) \right] - 5.6 + 20 \log \left(\frac{\sin\theta}{\sin(10°)} \right) \quad , \quad (2.1)$$

where
- d = effective grain diameter in meters,
- k = acoustic wave number in water, and
- θ = grazing angle.

2.2.2 Trapped Gas Bubbles

The trapped bubble component of the backscattering strength is based on resonance scattering from bubbles that exist in a fluid saturated porous medium. Acoustic propagation within the medium is modeled by the Biot theory. Bubble resonance behavior inside sediment pores is modeled via a simple modification to existing theory for bubbles surrounded by unbounded fluids.[2,19,20] In this modification, the pore fluid is assigned an effective density that differs from its actual density and accounts for the fluid's partial confinement. The details are described in Ref. 13.

Once the bubble scattering strength is known, an expression is developed for the backscattering strength per unit volume of sediment containing bubbles. An effective sediment interface scattering strength is obtained by assuming the backscatter from the interface is a sum of contributions from all volume elements below. The resulting expression for backscattering strength by bubbles is expressed in the following form.

8

$BS_b = 10 \log \times$

$$\left(\frac{\left(\dfrac{1}{r_{1m}^2}\right)\displaystyle\int_0^\infty |p_{1f} + p_{1s}|^2 \left[\dfrac{\sigma_{bvf}}{4\pi}\left(\dfrac{\rho_0 c_0}{\rho_{1f} c_{1f}}\right)|p_{1f}|^2 + \dfrac{\sigma_{bvs}}{4\pi}\left(\dfrac{\rho_0 c_0}{\rho_{1s} c_{1s}}\right)|p_{1s}|^2\right] dz}{|p_{inc}|^4} \right) , \quad (2.2)$$

where

σ_{bvf}	=	sediment volume scattering cross section - fast wave,
σ_{bvs}	=	sediment volume scattering cross section - slow wave,
p_{inc}	=	incident acoustic pressure,
p_{1f}	=	refracted acoustic pressure - fast wave,
p_{1s}	=	refracted acoustic pressure - slow wave,
ρ_0	=	fluid density above sediment,
ρ_{1f}	=	effective pore fluid density - fast wave,
ρ_{1s}	=	effective pore fluid density - slow wave,
c_0	=	sound speed in water column,
c_{1f}	=	fast wave sound speed,
c_{1s}	=	slow wave sound speed, and
z	=	depth below sediment interface.

2.2.3 Interface Roughness

The backscatter from interface roughness is modeled by solving the Helmholz-Kirchhoff integral. In this regard it is similar to the approach used by Jackson et al.[6] Both models use the Kirchhoff approximation which limits the frequency range of applicability. The applicable range has been estimated by Chotiros[21] for the measured roughness spectra of ocean sediments by Briggs.[22] However, the method adopted here is different from that of Jackson et al. in two important respects. (1) A numerical approach is used to compute the scattering

9

strength as a function of grazing angle, in order that measured wave number spectra of roughness from real ocean sediments, expressed in the form of a structure function, may be used. Jackson et al.,[6] on the other hand, attempted to fit a linear power law to measured wave number spectra. As a result, their ability to model was limited because the integral would only converge within a limited range of power law slopes. (2) The Biot theory is used to determine the sediment plane wave reflection coefficient whereas, in Jackson et al., the sediment is approximated as a fluid. When compared to measured values of reflection loss from ocean sediments, the Biot theory has been shown to give more realistic results. The plane wave backscattering strength, which is a simplified version of a result developed by Chotiros[21] for roughness scattering under more general conditions, is given by the following expression.

$$BS_r = 10 \log \left[\left| \int_{-\infty}^{\infty} \int_{-\infty}^{\infty} \left| \frac{kR}{2\pi} \sin(\theta) \right|^2 \exp\left\{ -2k^2 \left[D_z\left(\sqrt{x^2+y^2}\right)\sin^2(\theta) \right] + 2jkx \cos(\theta) \right\} dx\, dy \right| \right], \quad (2.3)$$

where

      k = acoustic wave number,

      θ = grazing angle,

      D_z = structure function of roughness, and

      R = plane wave reflection coefficient, a function of the grazing angle.

2.2.4 Total Backscattering Strength

The total backscattering strength is the incoherent sum of the above three components.

$$BS = 10 \log \left(10^{0.1\, BS_g} + 10^{0.1\, BS_b} + 10^{0.1\, BS_r} \right) \quad . \quad (2.4)$$

10

3. RUNNING BOGGART

In order to run, the BOGGART application must be accompanied by five input files. When the program is run, it will produce three output files. Input and output files are described in detail in Sections 3.1 and 3.2.

3.1 INPUT FILES

Input parameters for BOGGART are entered via input files which can be edited by the user. A file called "BOTTOM.INPUT" governs the program. An example is given in Fig. 3.1(a). This file selects four input files from which input parameters are gathered, as well as a user defined prefix which will be attached to all output files. In the example shown, all output file names will start with the prefix "test". The four input files selected by the user are (1) the sonar parameters file, (2) the sediment parameters file, (3) the structure function file, and (4) the sediment gas file.

An example sonar parameters file is shown in Fig. 3.1(b). The sonar frequencies and grazing angles are selected here. The quantity NTIMES is the number of frequencies to be selected. They will have logarithmic spacing between a minimum "FS4M" and a maximum "FS4X", inclusive. If NTIMES equals 1, then the modeled frequency will be the minimum 'FS4M'.

An example sediment parameters file is given in Fig. 3.2. This file contains the Biot parameters that describe the sediment. They are broken down into three groups: (1) solid parameters that describe the grain material, (2) fluid parameters that describe the pore fluid, and (3) frame parameters that describe the skeletal structure of the grain matrix. Four general sediment parameters files have been created to model different sediment types as follows.

Sediment Type	Name of Sediment Parameters File
coarse sand	sediment.sand1ø
medium sand	sediment.sand2ø
fine sand	sediment.sand3ø
mud	sediment.mud8ø

```
#File selections for BotBS3:
#Enter appropriate file names for input parameters and output results
sonar.parameters.file___ sonar.parameters
site.sediment.file_____ sediment.sand3ø
structure.function.file_ struct.sand9.5mmRMS
sediment.gas.file_____ gas.layers
output.file.prefix_____ test
#There will be 3 out put files with the above prefix
#NNN.BSfile will contain backscattering strength vs grazing angle
#NNN.const will contain a copy of all the input parameters
#NNN.vel will contain the wave velocities in the sediment
```

(a) Example of input file "BOTTOM.INPUT".

```
sonar parameters

'NTIMES-.NUMBER.OF.FREQUENCIES_____'  1
'FS4M-.MIN.FREQUENCY.<kHz>._____'  30.
'FS4X-.MAX.FREQUENCY.<kHz>._____'  30.
'NTHETA.-.NUMBER.OF.GRAZING.ANGLES_____'  10.
'THETMN-.MIN.GRAZING.ANGLE.<DEG>._____'  0.
'THETMX-.MAX.GRAZING.ANGLE.<DEG>._____'  90.
```

(b) Example of sonar parameters file.

Figure 3.1

12

```
sediment parameters: sand MGS= 3ø
Chotiros, 'Biot model of sandy sediments', submitted to JASA;
Boyle's dissertation
solid parameters
'RHOS-.SEDIMENT.GRAIN.DENSITY.<kg.m^-3>_'   2650.
'XKR-..SEDIMENT.GRAIN.BULK.MOD.<Pa>_____'  7.e9
'MEAN.GRAIN.PHI<MPHIs>_____'   3.0
'STAND.DEV.PHI<SIGPHIs>_____'   1.0

fluid parameters
'RHOF-.UPPER.FLUID.DENSITY.<kg.m^-3>_____'   1000
'XKF0-.UPPER.FLUID.BULK.MOD.<Pa>_____'   2.25e9
'RHOFBLO-.PORE.LIQUID.DENSITY.<kg.m^-3>_'    1000
'XKF0BLO-.PORE.LIQUID.BULK.MODULUS.<Pa>_'    2.25e9
'ETA-..PORE.LIQUID.VISCOSITY.<kg.m^-1.s>'    1.00e-3
'WATER.DEPTH<M>_____'   60.

frame parameters
'B-....SEDIMENT.POROSITY.<->_____'   .50
'XMU0-.SEDIMENT.FRAME.SHEAR.MOD..<Pa>___'    .261e+8
'DMU0-.SEDIMENT.FRAME.SHEAR.LOG.DECR.<->'    .15
'XKB0-.SEDIMENT.FRAME.BULK.MOD.<Pa>_____'   5.3e9
'DKB0-.SEDIMENT.FRAME.BULK.LOG.DECR..<->'    .15
'Vbp_____'    40.0
```

Figure 3.2
Example of sediment parameters file.

13

A user also has the option of creating a new sediment parameters file, if needed, and selecting it inside the BOTTOM.INPUT file.

Figure 3.3 is an example structure function file. In this file, sediment roughness parameters are specified. Two generic input files exist at present, which apply to different roughness scales:

rms Roughness	Name of Structure Function File
1.1 mm	struct.sand1.1mmRMS
9.5 mm	struct.sand9.5mmRMS

The user has the option of creating a new structure function file if necessary, and selecting it in the BOTTOM.INPUT file.

Figure 3.4 is an example of a sediment gas file. The first four entries describe the physical properties of the gas. At the bottom of the file is the layered gas fraction profile. Each row consists of the depth of the top of the layer, followed by the layer's gas fraction. The last layer is assumed to be an infinite half space. There is no limit to the number of layers which can be specified.

3.2 OUTPUT FILES

BOGGART produces three ASCII output files. The filenames consist of a prefix, specified by the user in the BOTTOM.INPUT file, and the suffix ".const", ".BS", or ".vel".

The "nnn.const" file is a readback of BOGGART's input parameters. An example is given in Fig. 3.5. The purpose of this file is to provide a complete record of the input parameter values.

The "nnn.BS" file is a table of computed backscattering strengths as a function of grazing angle and frequency. Figure 3.6(a) is an example. The first four lines are a list of the input files. The next two are a header, followed by the data, which are arranged in columns. The first column is the acoustic frequency

```
Sand:Briggs OCEAN ENG 1989 14(4),Mission bay II (isotropic)
without volume scatter
26            ! number of structure function samples in look up
table
0      0
0.000329222.5365E-09
0.000493835.6758E-09
0.000740741.2616E-08
0.001111112.7638E-08
0.001666675.88E-08
0.0025     1.1877E-07
0.00375    2.2481E-07
0.005625   4.1234E-07
0.0084375  7.5914E-07
0.012656251.3663E-06
0.018984382.3644E-06
0.028476563.8765E-06
0.042714845.897E-06
0.064072278.2724E-06
0.0961084 1.1138E-05
0.1441626 1.5345E-05
0.2162439 2.1896E-05
0.324365843.1934E-05
0.486548774.6889E-05
0.729823156.8196E-05
1.094734739.6382E-05
1.642102090.00012911
2.463153130.00015898
3.6947297 0.000176
5.542094550.00017976
```

Figure 3.3
Example of structure function file.

```
gas parameters: air, medium density

'JHcpg-SPEC.HEAT.OF.GAS..CONST.PRESSURE_ '  0.629
'JHrhog-GAS.DENSITY.<kg.m^-3>_____ '  1.22
'XKG-..GAS.BULK.MOD..<Pa>_____ '  2.48e5
'DEPTH.OF.TOP.OF.LAYER.(M),GAS.FRACTION:'
0.0,1E-3
0.1,1E-5
```

Figure 3.4
Example of sediment gas parameters file.

16

```
description(NO SLASHES,SPACES OR COMMAS)data field
File.Name.of.out.put.results_____test
sonar parameter input file_____ sonar.parameters
sediment site input file_____ sediment.sand3ø
sediment structure input file__ struct.sand9.5mmRMS
gas parameter input file_____ gas.layers


solid parameters
RHOS-..SEDIMENT.GRAIN.DENSITY.(kg.m^-3)_  2650.00
XKR-...SEDIMENT.GRAIN.BULK.MOD.(Pa)_____  7.000000E+09
MEAN.GRAIN.PHI(rphis)_____  3.00000
STAND.DEV.PHI(dphis)_____  1.00000

fluid parameters
RHOF-.UPPER.FLUID.DENSITY.(kg.m^-3)_____  1000.00
XKF0-.UPPER.FLUID.BULK.MOD.(Pa)_____  2.250000E+09
RHOFBLO-.PORE.LIQUID.DENSITY.(kg.m^-3)_  1000.00
XKF0BLO-.PORE.LIQUID.BULK.MODULUS.(Pa)_  2.250000E+09
ETA-..PORE.LIQUID.VISCOSITY.(kg.m^-1.s)  1.000000E-03
WATER.DEPTH_____  60.0000

gas parameters
JHcpg-SPEC.HEAT.OF.GAS..CONST.PRESSURE_  1000.00
JHckg-HEAT.CONDUCTIVITY.GAS_____  .629000
JHrhog-GAS.DENSITY.(kg.m^-3)_____  1.22000
XKG-..GAS.BULK.MOD..(Pa)_____  248000.
Vbp_____  40.0000

frame parameters
B-....SEDIMENT.POROSITY.(-)_____  .500000
XMU0-.SEDIMENT.FRAME.SHEAR.MOD..(Pa)___  2.610000E+07
DMU0-.SEDIMENT.FRAME.SHEAR.LOG.DECR.(-)  .150000
XKB0-.SEDIMENT.FRAME.BULK.MOD.(Pa)_____  5.300000E+09
DKB0-.SEDIMENT.FRAME.BULK.LOG.DECR..(-)  .150000

dependent constants
B-....SEDIMENT.POROSITY.(-)_____  .500000
VMASS-..VIRTUAL.MASS.CONSTANT.(-)_____  1.50000
PERM-...PERMEABILITY(m^2)_____  1.134527E-10
aa-....PORE.SIZE.PARAMETER.(m)_____  6.736548E-05
CC-....CONSTITUENT.PARAMETER.C_____  (1.313699E+09,1.583202E+08)
CH-....CONSTITUENT.PARAMETER.H_____  (5.648118E+09,-1.687774E+08)
CM-....CONSTITUENT.PARAMETER.M_____  (5.387022E+09,-1.499875E+08)

independent variables
NTIMES-NUMBER.OF.FREQUENCIES_____  1
FS4M-MINIMUM.FREQUENCY(kHz)_____  30.0000
FS4X-MAXIMUM.FREQUENCY(kHz)_____  30.0000
NTHETA.-NUMBER.OF.GRAZING.ANGLES_____  10
THETMN.-MINIMUM.GRAZING.ANGLE.DEG_____  .000000
THETMX.-MAXIMUM.GRAZING.ANGLE.DEG_____  90.0000
Gassy layers: top boundary and gas fraction
number of gassy layers___  2
      .000000  1.000000E-03
      .100000  1.000000E-05
Structure function (m,m^2)
number of structure function samples___  26
      .000000   .000000
    3.292200E-04  2.536500E-09
    4.938300E-04  5.675800E-09
    7.407400E-04  1.261600E-08
    1.111110E-03  2.763800E-08
    1.666670E-03  5.880000E-08
    2.500000E-03  1.187700E-07
    3.750000E-03  2.248100E-07
    5.625000E-03  4.123400E-07
    8.437500E-03  7.591400E-07
    1.265625E-02  1.366300E-06
    1.898438E-02  2.364400E-06
    2.847656E-02  3.876500E-06
    4.271484E-02  5.897000E-06
    6.407227E-02  8.272400E-06
    9.610840E-02  1.113800E-05
    .144163  1.534500E-05
    .216244  2.189600E-05
    .324366  3.193400E-05
    .486549  4.688900E-05
    .729823  6.819600E-05
    1.09473  9.638200E-05
    1.64210  1.291100E-04
    2.46315  1.589800E-04
    3.69473  1.760000E-04
    5.54209  1.797600E-04
```

Figure 3.5
Example output file "test.const": list of input parameter values.

17

```
sonar parameter input file_____ sonar.parameters
sediment site input file_____ sediment.sand3ø
sediment structure input file__ struct.sand9.5mmRMS
gas parameter input file_____ gas.layers
FREQ      |G ANGL|FORWARD|  BACKSCATTERING STRENGTH(dB)
 kHz      | deg  LOSS dB   deg.    TOTAL     GAS   GRAINS  ROUGH X
  30.000   .0       .00 -180.00 -100.00    -INF    -INF -100.00 ROUGHNESS
  30.000 10.0     -8.49 -123.32  -19.15  -19.15  -74.27 -100.00 GAS
  30.000 20.0    -11.26  -59.81  -13.31  -13.31  -68.38  -91.09 GAS
  30.000 30.0    -10.73  -22.37  -11.08  -11.08  -65.09  -76.09 GAS
  30.000 40.0    -11.79   -1.00  -10.36  -10.36  -62.90  -50.40 GAS
  30.000 50.0    -12.68     .84  -10.11  -10.11  -61.38  -45.15 GAS
  30.000 60.0    -12.86    1.00   -9.81   -9.82  -60.31  -37.84 GAS
  30.000 70.0    -12.90    1.04   -9.60   -9.64  -59.61  -29.69 GAS
  30.000 80.0    -12.90    1.05   -9.22   -9.50  -59.20  -21.37 GAS
  30.000 90.0    -12.89    1.05   11.65   -9.45  -59.07   11.62 ROUGHNESS
```

(a) Example output file "test.BS": backscattering strengths.

```
at (1.57080,.000000)degrees grazing and  30.0000kHz:

fast.wavespeed(VEL1o)_____ 1877.46
slow.wavespeed(VEL2o)_____ 1288.32
shear.wavespeed(VELso)_____ 131.239
fast.absorption(ABSRP1o)_____ 34.3029
slow.absorption(ABSRP2o)_____ 59.1957
shear.absorption(ABSRPSo)_____ 398.683
```

(b) Example output file "test.vel": predicted sediment sound speeds
and absorptions in m/s and dB/m.

Figure 3.6

in kHz. The second is the grazing angle in degrees. The third and fourth columns are the forward loss and phase angle of the reflection coefficient. The next four columns are backscattering strengths in dB; the fifth column is the total predicted backscattering strength, followed by the individual backscattering strength components for trapped gas, sediment grain, and interface roughness scattering. In the ninth column, the dominant scattering mechanism is specified: either "gas", "grains", or "roughness".

The "nnn.vel" file, shown in Fig. 3.6(b), is a list of computed sound speeds and attenuations within the sediment. They are based on the Biot theory and therefore include values for fast, slow, and shear waves. The purpose of this file is to provide acoustic wave speeds and attenuations within the sediment which may be useful in understanding the paths by which the sound energy engages the scattering mechanisms.

This page intentionally left blank.

4. BOGGART MODEL STRUCTURE

BOGGART is written in FORTRAN. It consists of the driver BotBS6 and 22 subroutines as illustrated in Fig. 4.1. The subprograms perform the following functions.

BotBS6:   Serves as the driver for BOGGART. BotBS6 opens input files and calls subroutines DATREAD3, GASREAD, and STRCTREAD to read them. It then calls subroutines BIOTK, SANDBS, SURFBS, GRAINBS, and ROUGBS to perform computations and write the results to the appropriate output files.

DATREAD3:   Reads in all input parameters, except those describing the trapped gas or the interface roughness.

GASREAD: Reads in parameters pertaining to the trapped gas, such as its density and bulk modulus.

STRCTREAD: Reads in parameters that describe the interface roughness.

BIOTK: Calculates wave numbers, sound speeds, and attenuations associated with Biot fast and slow waves in the sediment pore fluid. It calls four other subroutines: GASMOD, INITCON2, TXRCOF, and RHOEF.

GASMOD: This routine exists for the future incorporation of an algorithm to compute the bulk modulus of a gassy fluid. At present no computations occur in GASMOD, although two variables used elsewhere in BOGGART are defined. CKM is the complex compressibility of the bubbly pore fluid, presently set equal to the real compressibility of the fluid without bubbles. RHOM is the density of the bubbly fluid, presently set equal to the compressibility of the fluid without bubbles.
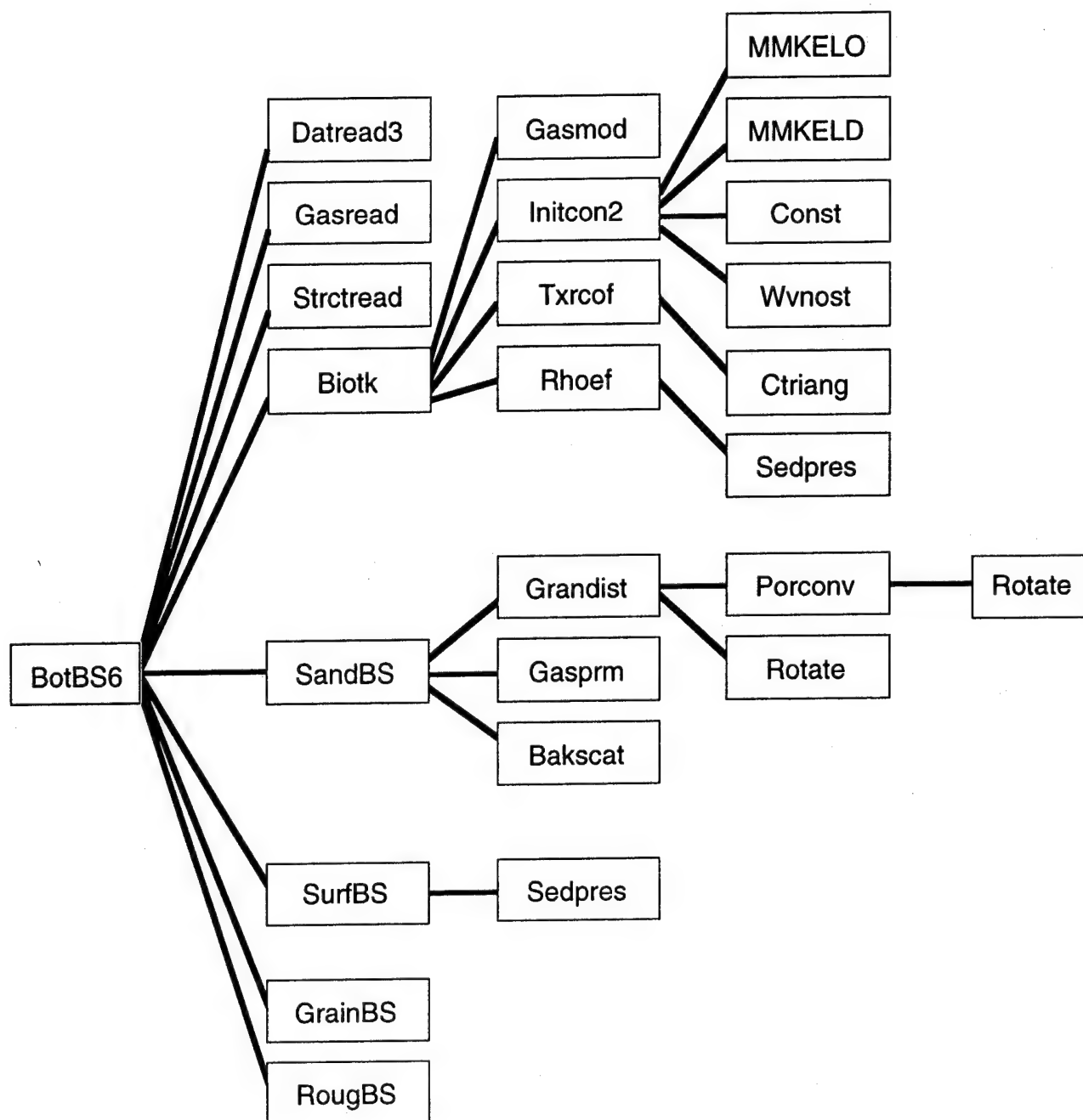
Figure 4.1
BOGGART program structure.

INITCON2: This routine contains the Biot model's computations. It calls three other subroutines: MMKEL0, MMKELD, and CONST.

MMKEL0: Calculates the Kelvin functions ber(x) and bei(x) required in Biot model.

MMKELD: Calculates the Kelvin function derivatives ber'(x) and bei'(x) required in Biot model.

CONST: Calculates some of the constants which are carried through the Biot equations.

WVNOS: Calculates vertical components of the complex wave numbers of the fast, slow, and shear waves within the sediment. They are assigned the names "CL1", "CL2", and "CLS", respectively.

TXRCOF: Calculates Biot transmission and reflection coefficients by Gaussian elimination of the linear equations (51)-(54) in Ref. 14. Calls subroutine CTRIANG.

CTRIANG: Triangulates a complex matrix of dimension M×M.

RHOEF: Calculates fast and slow wave effective densities of the pore fluid by solution of Eqs. (37) and (38) in Ref. 13. It calls the subroutine SEDPRES.

SEDPRES: Calculates sediment normal tractions and pore fluid pressures at the fluid/sediment boundary.

SANDBS: Finds the volume backscattering cross sections σ_{bvs} and σ_{bvf}, given the appropriate pore fluid effective density calculated by the subroutine RHOEF.

GRANDIST: Calculates shape of bubble size distribution from measured grain size distribution. The result is entered into an array called "BUBPOP". This array is not normalized. The total volume of gas subtended by BUBPOP, per volume of pore fluid, is assigned the name INTGR. Calls subroutines PORCONV, ROTATE.

PORCONV: Calculates pore size density function by convolving grain size density function with a pore size density function of a dense random packing of hard spheres, according to Eq. (14) in Ref. 13.

ROTATE: Rotates a real one-dimensional array of "NARRAY" data points by "NROT" points.

GASPRM: Normalizes BUBPOP to obtain a bubble size density function called BPNORM, whose total gas volume equals the sediment porosity.

BAKSCAT: Finds the backscattering strength per unit volume of sediment. BAKSCAT is called twice inside SANDBS, once for the Biot fast wave and once for the slow wave.

SURFBS: Finds effective backscattering strength of sediment interface by summing contributions from the sediment volume below. The sediment volume is broken up into depth cells, from which contributions are summed.

SURFBS: Adjusts the depth increment of the cells so that the Biot wave with the fastest decay rate decreases its pressure amplitude by 10% from the top to the bottom of a single cell. The integration is carried to a depth determined by the pressure amplitude of the wave with the slowest decay rate. When this wave has 10% of its amplitude at the interface, the integration is stopped. If a medium with multiple layers is modeled, the integration is not allowed to stop until the last layer is reached.

SURFBS: Calls one other subroutine, "SEDPRES" to get the refracted acoustic pressures at the water/sediment interface.

GRAINBS: Calculates the backscattering strength contribution due to scattering from sediment grains. Empirical modeling, based on the experiments of Nolle et al.,[3] is currently used in lieu of a theoretical model, which is under development.

ROUGBS: Calculates the backscatter component due to interface roughness by evaluation of the Helmholz-Kirchhof integral.

This page intentionally left blank.

REFERENCES

1. R. E. Patterson, "Backscatter of Sound from a Rough Boundary," J. Acoust. Soc. Am. 35, 2010-2013 (1963).

2. C. S. Clay and H. Medwin, *Acoustical Oceanography: Principles and Applications* (Wiley-Interscience, New York, 1977).

3. A. W. Nolle, W. A. Hoyer, J. F. Mifsud, W. R. Runyan, and M. B. Ward, "Acoustic Properties of Water-Filled Sands," J. Acoust. Soc. Am. 35, 1394 (1963).

4. J. H. Stockhausen, "Scattering from the Volume of an Inhomogeneous Half-Space," NRE Report No. 63/9, Naval Research Establishment, Nova Scotia, 1963.

5. A. N. Ivakin and Yu. P. Lysanov, "Underwater Sound Scattering by Volume Inhomogeneities of a Bottom Medium Bounded by a Rough Surface," Sov. Phys. Acoust. 27, 212-215 (1981).

6. D. R. Jackson, D. P. Winebrenner, and A. Ishimaru, "Application of the Composite Roughness Model to High-Frequency Bottom Backscattering," J. Acoust. Soc. Am. 79, 1410-1422 (1986).

7. P. D. Mourad and D. R. Jackson, "High-Frequency Sonar Equation Models for Bottom Backscatter and Forward Loss," in *Proceedings of Oceans '89*, 1168-1175.

8. D. R. Jackson and K. B. Briggs, "High-Frequency Bottom Backscattering: Roughness versus Interface Scattering," J. Acoust. Soc. Am. 92, 962-977 (1992).

9. N. P. Chotiros and F. A. Boyle, "Gas Bubbles in Ocean Sediments and High-Frequency Acoustic Backscattering Strength," presented at 121st Meeting of the Acoustical Society of America; J. Acoust. Soc. Am. 89(4), Pt. 2, 1852 (1991).

10. N. P. Chotiros and H. Boehme, "Analysis of Bottom Backscatter Data from the Kings Bay Experiment," Applied Research Laboratories Technical Report No. 88-6 (ARL-TR-88-6), Applied Research Laboratories, The University of Texas at Austin, 29 January 1988.

11. N. P. Chotiros, "High Frequency Bottom Backscattering: Panama City Experiment," Applied Research Laboratories Technical Report No. 90-22 (ARL-TR-90-22), Applied Research Laboratories, The University of Texas at Austin, 25 July 1990.

12. F. A. Boyle and N. P. Chotiros, "Experimental Detection of a Slow Acoustic Wave in Sediment at Shallow Grazing Angles," J. Acoust. Soc. Am. 91, 2615-2619 (1992).

13. F. A. Boyle and N. P. Chotiros, "A Model for High-Frequency Acoustic Backscatter from Gas Bubbles in Sandy Sediments at Shallow Grazing Angles," J. Acoust. Soc. Am. 98(1), 531-541 (1995).

14. M. Stern, A. Bedford, and H. R. Millwater, "Wave Reflection from a Sediment Layer with Depth-Dependent Properties," J. Acoust. Soc. Am. 77, 1781-1788 (1985).

15. D. J. Yelton and N. P. Chotiros, "New Multiple Scatter Model of the Ocean Sediment," presented at 129th Meeting of the Acoustical Society of America; J. Acoust. Soc. Am. 97(5), Pt. 2, 3387 (1995).

16. M. A. Biot, "Theory of Propagation of Elastic Waves in a Fluid Saturated Porous Solid. I. Low Frequency Range," J. Acoust. Soc. Am. 28, 168-178 (1956).

17. M. A. Biot, "Theory of Propagation of Elastic Waves in a Fluid Saturated Porous Solid. II. Higher Frequency Range," J. Acoust. Soc. Am 28, 179-191 (1956).

18. N. P. Chotiros, "Biot Model of Sound Propagation in Water-Saturated Sand," J. Acoust. Soc. Am. 97(1), 199-214 (1994).

19.   M. Minnaert, "On Musical Air-Bubbles and the Sounds of Running Water," Phil. Mag. 26, 235 (1933).

20.   C. Devin, "Survey of Thermal, Radiation, and Viscous Damping of Pulsating Air Bubbles in Water," J. Acoust. Soc. Am. 31, 1654-1667 (1959).

21.   N. P. Chotiros, "Reflection and Reverberaton in Normal Incidence Echo-Sounding," J. Acoust. Soc. Am. 96(5), 2921-9 (1994).

22.   K. B. Briggs, "Microtopographical Roughness of Shallow-Water Continental Shelves," IEEE J. Oceanic Eng. 14(4), 360-367 (1989).

REFERENCES, FIG. 2.1:

23.   J. L. Jones, C. B. Leslie, and L. E. Barton, "Acoustic Characteristics of Underwater Bottoms," J. Acoust. Soc. Am. 36(1) 154-157 (1964).

24.   D. J. Dodds, "Attenuation Estimates from High Resolution Subbottom Profiler Echoes," in Bottom-Interacting Ocean Acoustics, W. A. Kuperman, and F. B. Jensen (eds.), NATO Conference Series IV (Marine Sciences, Plenum Press, New York, 1980, pp. 525-540.

25.   N. P. Chotiros, "Inversion and Sandy Ocean Sediments," in Full Field Inversion Methods in Ocean and Seismo-Acoustics, O. Diachok, A. Caiti, P. Gerstoft, and H. Schmidt (eds.), 353-357, Modern Approaches in Geophysics, Vol. XII (Kluwer Academic Publishers, Dordrecht, 1995), pp. 353-357.

This page intentionally left blank.

DISTRIBUTION LIST
ARL-TR-95-27
**Technical Report under Contract N00039-91-C-0082,
TD No. 01A2049, Sensor and Environmental Support for MTEDS**

<u>Copy No.</u>

	Commanding Officer
	Naval Research Laboratory
	Stennis Space Center, MS 39529-5004
1-3	Attn: S. Tooma (Code 7430)
4	D. Lott (Code 7431)
5	E. Franchi (Code 7100)
6	S. Stanic (Code 7174)
7	D. Ramsdale (Code 7170)
8	M. Richardson (Code 7431)
9	R. Meredith (Code 7174)
10	Library (Code 7032.2)

Office of Naval Research
San Diego Regional Office
4520 Executive Drive, Suite 300
San Diego, CA 92121-3019
11   Attn: J. Starcher, ACO

Director
Naval Research Laboratory
Washington, DC 20375
12   Attn: Code 2627
13   B. Houston (Code 5136)

DTIC-OCC
Defense Technical Information Center
8725 John J. Kingman Road, Suite 0944
Fort Belvoir, VA 22060-6218
14 - 25   Attn: Library

Director
Research Program Department
Office of Naval Research
Ballston Tower One
800 North Quincy Street
Arlington, VA 22217-5000
26   Attn: J. Simmen (Code 321)
27   E. Chaika (Code 322)
28   W. Ching (Code 321)
29   T. Goldsberry (Code 322)
30   D. Houser (Code 333)

<u>Copy No.</u>

	Commander Naval Meteorology and Oceanography Command 1020 Balch Boulevard Stennis Space Center, MS 39529
31	Attn: D. Durham (Code N5A)
32	R. Martin (Code N5C)

	Commander Program Executive Office - Mine Warfare Crystal Plaza Bldg 6 2531 Jefferson Davis Highway Arlington, VA 22242-5167
33	Attn: J. Grembi (PEOMIW)
34	D. Gaarde (PMO407B)

	G & C Systems Manager MK48/ADCAP Program Office National Center 2 2521 Jefferson Davis Hwy., 12W32 Arlington, VA 22202
35	Attn: H. Grunin (PMO402E1)

	Program Manager MK50 Torpedo Program Office Crystal Park 1 2011 Crystal Drive, Suite 1102 Arlington, VA 22202
36	Attn: A. Knobler (PMO406B)

	Commander Dahlgren Division Naval Surface Warfare Center Dahlgren, VA 22448-5000
37	Attn: Library

Copy No.

Director
Applied Physics Laboratory
The University of Washington
1013 NE 40th Street
Seattle, WA 98105
38   Attn: R. Spindel
39   D. Jackson
40   K. Williams
41   S. Kargl

Director
Life Sciences Directorate
Office of Naval Research
Arlington, VA 22217-5000
42   Attn: S. Zornetzer (Code 114)

Director
Marine Physical Laboratory
The University of California, San Diego
San Diego, CA 92152
43   Attn: K. Watson
44   C. De Moustier

Commander
Mine Warfare Command
325 Fifth St. SE
Corpus Christi, TX 78419-5032
45   Attn: G. Pollitt (Code N02R)

Applied Research Laboratory
The Pennsylvania State University
P.O. Box 30
State College, PA 16804-0030
46   Attn: R. Hettche
47   R. Goodman
48   E. Liszka
49   Library
50   D. McCammon
51   F. Symons

<u>Copy No.</u>

Commanding Officer
Coastal Systems Station, Dahlgren Division
Naval Surface Warfare Center
Panama City, FL 32407-5000
52   Attn: M. Hauser (Code 10CD)
53   R. Lim (Code 130B)
54   E. Linsenmeyer (Code 10P)
55   D. Todoroff (Code130)

Commander
Naval Undersea Warfare Center Division
New London, CT 06320-5594
56   Attn: J. Chester (Code 3112)
57   P. Koenig (Code 33A)

Advanced Research Projects Agency
3701 North Fairfax Drive
Arlington, VA 22203-1714
58   Attn: W. Carey

Commander
Naval Undersea Warfare Center Division
Newport, RI 02841-5047
59   Attn: J. Kelly (Code 821)
60   F. Aidala (Code 842)
61   W. Gozdz (Code 843)

National Center for Physical Acoustics
University of Mississippi
Coliseum Drive
University, MS 38677
62   Attn: J. Sabatier

Physics Department
The University of Texas at Austin
Austin, TX 78712
63   Attn: T. Griffy

Aerospace Engineering Department
The University of Texas at Austin
Austin, TX 78712
64   Attn: M. Bedford
65   M. Stern

Distribution List for ARL-TR-95-27 under Contract N00039-91-C-0082, TD No. 01A2049 (cont'd)

<u>Copy No.</u>

66	Robert A. Altenburg, ARL:UT
67	Hollis Boehme, ARL:UT
68	Frank A. Boyle, ARL:UT
69	Nicholas P. Chotiros, ARL:UT
70	John M. Huckabay, ARL:UT
71	Thomas G. Muir, ARL:UT
72	Library, ARL:UT
73 - 77	Reserve, Advanced Sonar Group, ARL:UT